Local environment of Mn dopant in ZnO by near-edge x-ray absorption fine structure analysis

Masahiro Kunisu, Fumiyasu Oba, Hidekazu Ikeno, and Isao Tanaka[a)]
Department of Materials Science and Engineering, Kyoto University, Yoshida, Sakyo, Kyoto 606-8501, Japan

Tomoyuki Yamamoto
Fukui Institute for Fundamental Chemistry, Kyoto University, Takano, Sakyo, Kyoto 606-8103, Japan

(Received 20 September 2004; accepted 31 January 2005; published online 14 March 2005)

High-resolution near-edge x-ray absorption fine structure (NEXAFS) at Mn *K* edge is employed to probe the local environment of Mn dopant in ZnO. First-principles supercell calculations are systematically made to obtain theoretical NEXAFS. Mn is found to substitute for Zn up to 5 at.% Mn in polycrystalline samples sintered at 1623 K in air. Presence of Mn_3O_4 is apparent for samples with higher Mn content. The NEXAFS does not change in the range of Mn concentration from 0.01 to 5 at. %, indicating the absence of Mn precipitates. The results are confirmed by examining the polarization dependence of the NEXAFS for a 5 at. %-doped ZnO thin film. © *2005 American Institute of Physics*. [DOI: 10.1063/1.1885175]

Semiconductors doped with dilute magnetic elements, now referred to as diluted magnetic semiconductors (DMSs), have been extensively studied since the discovery of carrier-induced ferromagnetism in $In_{1-x}Mn_xAs$[1] and $Ga_{1-x}Mn_xAs$.[2] Effort has been devoted to explore systems with higher Curie temperature by changing both dopants and matrix semiconducting materials. Recent calculations based on the Zener model of ferromagnetism predicted that Mn-doped GaN and ZnO can have a T_c higher than room temperature.[3] Supporting this prediction, high T_c above room temperature has been attained in Mn-doped ZnO.[4–6] However, ferromagnetism with T_c below room temperature,[7] paramagnetism,[8] and spin-glass behavior[9] were also reported in this system. Additionally, a recent report on Mn-doped ZnO indicates that the precipitation of Mn may result in the disappearance of ferromagnetism.[4] For the detailed understanding of the magnetic properties, it is essential to know the environment of the doped transition elements on an atomic scale. In this letter we report the local environment of Mn dopant in ZnO polycrystals and a thin film determined from near-edge x-ray absorption fine structures (NEXAFS) at Mn *K* edge in conjunction with first-principles calculations. We have previously shown that this approach can reveal the local environment of ultra dilute dopants at a concentration level of several at.p.p.m.[10] In order to investigate Mn dopants in ZnO, the NEXAFS at Mn *L*-edge has so far been used,[11] but to our best knowledge there is no report on Mn *K*-edge NEXAFS of Mn doped ZnO.

Polycrystalline specimens of ZnO:Mn were fabricated by mixing commercially available high-purity powder of MnO_2 (Soekawa Chemical Co. Ltd.) with ZnO powder (Rare Metallic Co. Ltd.) when the Mn concentrations of 3, 5, 10, and 20 at.%. For the dilute specimens with Mn concentration of 0.01, 0.1, and 1 at.%, Mn nitrate hexahydrate (Soekawa Chemical Co. Ltd.) was mixed with ZnO powder (Rare Metallic Co. Ltd.) in ethanol using a Teflon-coated magnetic stirrer until they dried up. All of these powders were isostatically pressed into a pellet at 100 MPa, sintered in air at 1623 K for 3 h, and cooled at 225 K/h. The Mn-doped ZnO thin film was prepared by a pulsed laser deposition (PLD) using an excimer KrF* laser source ($\lambda = 248$ nm, $\tau = 25$ ns, Lambda Physik COMPex2005). The laser power was $\sim 3 \times 10^4$ J m^{-2}. $Al_2O_3(0001)$ single crystal was used for the substrate, which was kept at 873 K during the deposition. 1 Hz laser was irradiated for 5000 shots, which yielded approximately ZnO:Mn thin film with 100 nm thickness. A PLD target with 5 at.% Mn was fabricated in the same manner as the above polycrystalline specimens.

The NEXAFS measurements were carried out at BL01B1 in SPring8, Harima, Japan. The polycrystalline specimens with the dopant concentrations above 1 at.% were measured in the transmission mode. On the other hand, the total fluorescence yield (TFY) mode using the 19 elements Ge solid-state detector was chosen for the polycrystalline specimens with the dopant concentrations of 1 at.% or less and a thin film sample. The x-rays were monochromatized by the Si(111) double-crystal monochrometer and irradiated perpendicularly onto the sample surface in the case of transmission mode and 45° normal to the sample surface in the case of TFY measurements of polycrystalline specimens. For a thin film sample, TFY mode was chosen for efficiency, in which two kinds of geometries were used to see the polarization dependence of the spectra. The method is identical to that we previously used for rock-salt structured $Zn_xMg_{1-x}O$ thin films with slight tetragonal distortion,[12] i.e., $\boldsymbol{E} \parallel \boldsymbol{T}$ and $\boldsymbol{E} \perp \boldsymbol{T}$, where $\boldsymbol{E}$ is the electric field vector and $\boldsymbol{T}$ is the vector perpendicular to the surface of the thin film. NEXAFS spectra of commercially available high-purity powders of MnO and Mn_3O_4 diluted by mixing with BN powders were also measured for reference.

Prior to the NEXAFS measurements all the samples were characterized by the x-ray diffraction (XRD) technique with θ-2θ scan, in which Cu $K\alpha$ x-rays was employed. The results are shown in Fig. 1 for the Mn-doped ZnO polycrystals with Mn concentrations of 5, 10, and 20 at.% and the

a)Author to whom correspondence should be addressed; electronic mail: isao.tanaka@materials.mbox.media.kyoto-u.ac.jp

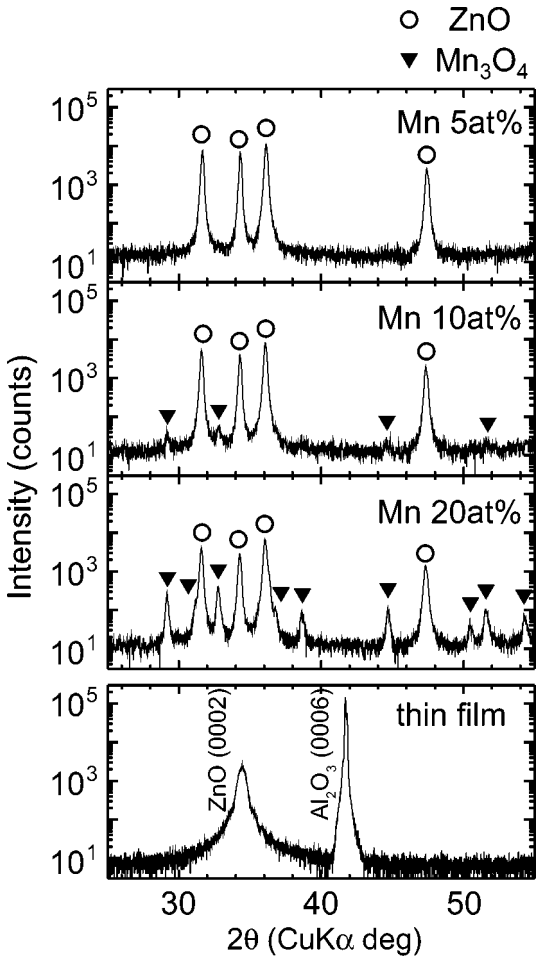

FIG. 1. XRD patterns of Mn-doped polycrystals with 5, 10, and 20 at.%Mn and a thin film with 5 at.%Mn.

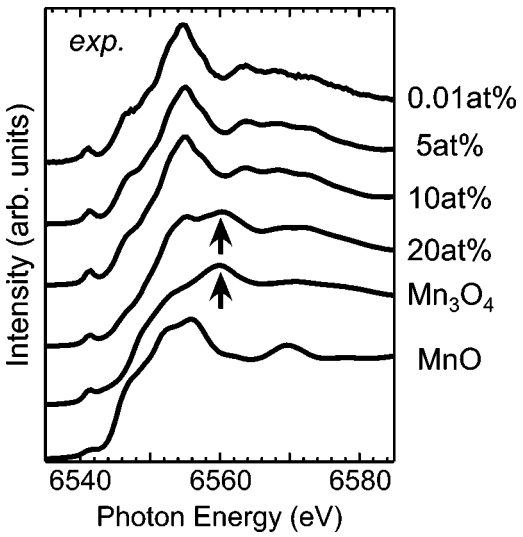

FIG. 2. Observed NEXAFS spectra of Mn *K* edge from polycrystalline ZnO:Mn specimens with Mn concentrations of 0.01, 5, 10, and 20 at.%. The spectra from MnO and Mn_3O_4 reference materials are also shown with characteristic peaks arrowed.

thin film. No diffraction peaks can be found except for those of the wurtzite structured ZnO in the XRD pattern of ZnO:Mn polycrystals at the Mn concentration of 5 at.%. Similar patterns were obtained for Mn concentrations less than 5 at.%. On the other hand, some additional diffraction peaks originating from Mn_3O_4 are present in the case of ZnO:Mn with 10 at.%Mn. At 20 at.%Mn, additional diffraction peaks of Mn_3O_4 are clearly seen. It is noted that no peaks of MnO and MnO_2 were found at all Mn concentrations. These XRD results suggest that the maximum solubility of Mn in ZnO via our processing is between 5 and 10 at.%. In the XRD pattern of the thin film, only one peak originating from the wurtzite structured ZnO (0002) is recognized except for the diffraction from the substrate of Al_2O_3(0006), which suggests that this thin film is highly oriented along the *c*-axis of wurtzite structured ZnO. However, it is not possible to know how Mn dopants are present within ZnO crystals only from these XRD results.

Observed NEXAFS spectra of polycrystalline ZnO:Mn specimens at Mn *K*-edge are shown in Fig. 2. The Mn *K*-edge NEXAFS profiles show almost the same features at the Mn concentrations between 0.01 and 5 at.%. The NEXAFS feature of ZnO:Mn with 10 at.%Mn is also very similar to the ones with lesser concentrations, whereas a very small amount of Mn_3O_4 was found in XRD pattern when plotted in a logarithmic scale. These results suggest that Mn dopants are mostly dissolved in ZnO and a minor portion exists as Mn_3O_4 at 10 at.%Mn. At a higher Mn concentration of 20 at.%, change in NEXAFS shape is clearly recognized. The spectrum can be described by the sum of the spectra of a reference Mn_3O_4 and ZnO:Mn with a lower concentration, indicating a significant amount of Mn is present as Mn_3O_4.

The NEXAFS spectrum has not been reported for the ZnO:Mn system at Mn *K*-edge. Hence, first-principles spin-polarized density functional theory (DFT) calculations were carried out to confirm that the NEXAFS spectra of ZnO:Mn (at Mn *K*-edge) originated from the substitutional Mn at Zn sites in ZnO. The full-potential augmented plane wave plus local orbitals (APW+lo) package, WIEN2k,[13] was employed with the generalized gradient approximation proposed by Perdew *et al.*[14] The muffin-tin radii, R_{MT}, of Zn, Mn, and O were set to 1.75 a.u., and the product of R_{MT} and $K_{\max}$, which corresponds to the plane wave cutoff, was set to 6.0(a.u. $Ry^{1/2}$) for all calculations. In these calculations, core-hole effects were fully introduced by removing one electron from the Mn *K* shell of our interest and putting additional electron in the conduction band, which approximately corresponds to the final state of the x-ray absorption process. A supercell consisting of 108 atoms was constructed by expanding the unit cell of ZnO by three times along each axis ($3\times3\times3$), respectively, in which one Zn atom was replaced by a Mn atom. Geometry change due to the substitution of Mn was not taken into consideration.[15] Theoretical NEXAFS spectrum of Mn_3O_4 was also obtained by using a 112-atom supercell in the same manner, where experimentally reported ferrimagnetic ordering[16] was assumed. A theoretical spectrum was obtained as a product of dipole allowed radial matrix element and the corresponding projected partial density of states, which was broadened with the Gaussian function of $\Gamma=1.0$ eV full width at half maximum. Transition energy was obtained as a difference in the total electronic energies of the core-hole (final) and the ground (initial) states. The resultant theoretical NEXAFS spectra of Mn_3O_4 and ZnO:Mn at Mn *K*-edge are compared with experimental ones in Fig. 3(a) and 3(b), respectively. The experimental spectral fine structures for ZnO:Mn system up to the solute concentrations of 5 at.% are well reproduced by the present

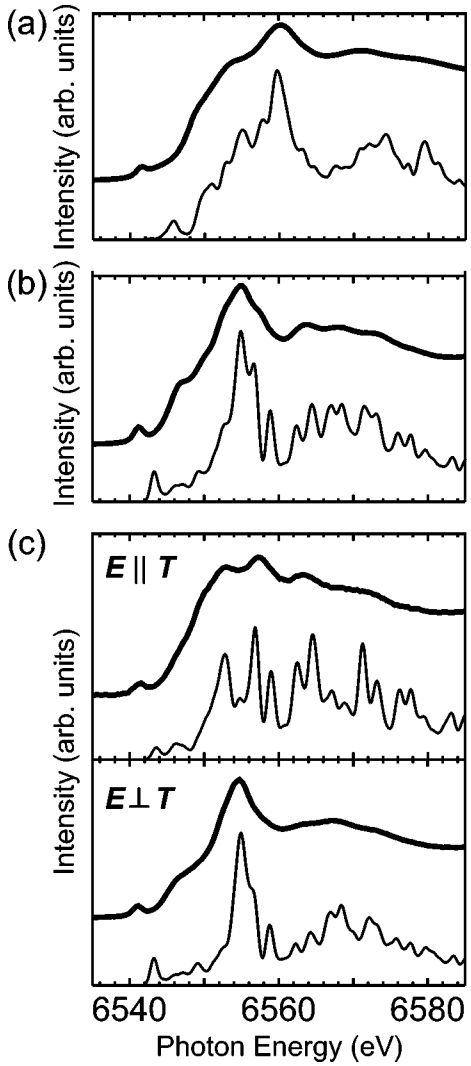

FIG. 3. Comparison of NEXAFS spectra between calculations and experiments for (a) Mn_3O_4, Mn-doped ZnO, (b) polycrystal, and (c) thin film. ***E*** and ***T*** are the electric field vector and the vector perpendicular to the surface of the thin film, respectively. Thick and thin solid curves are experiments and calculations, respectively. Absolute transition energies of all theoretical spectra were shifted by −20 eV ($\Delta E/E=0.3\%$).

first-principles calculations when the absolute transition energy are corrected by $\Delta E=20$ eV($\Delta E/E=0.3\%$). Difference in spectral fine structures and energies of the most intense peaks between the theoretical spectra of Mn_3O_4 and ZnO:Mn is clearly distinguishable. This comparison can lead to the conclusion that the NEXAFS spectrum of Mn in ZnO originates from substitutional Mn dopant at Zn site in ZnO. Although a recent report on ZnO:Mn polycrystals claimed the presence of Mn precipitates when specimens were sintered at 973 K or higher,[4] our NEXAFS and first-principles results with the assistance of XRD disagree to their results. Mn can completely substitute for Zn in the ZnO specimens sintered at 1623 K.

The NEXAFS spectra of a Mn-doped ZnO thin film obtained with two different geometries are shown in Fig. 3(c). Significant difference between these two NEXAFS spectra can be seen. This results show that the thin film is highly oriented as suggested by XRD. In order to confirm the polarization dependence of these NEXAFS spectra, theoretical spectrum for ZnO:Mn shown in Fig. 3(b) was decomposed into two components, i.e., parallel and perpendicular to the *c* axis of the wurtzite phase. Two theoretical spectra are compared with the experiments in Fig. 3(c). Both of the experimental spectra are satisfactory reproduced by assuming ***T*** is parallel to the *c* axis of ZnO. These agreements in the spectral shape clearly confirm that Mn is located at Zn site in the wurtzite structured ZnO thin film.

In conclusion, we have investigated the local environments of Mn dopant in ZnO polycrystals and a thin film by combining the high-resolution NEXAFS technique and first-principles calculations. The spectral fine structures indicate that Mn is located at Zn site up to the concentrations of 5 at.% in polycrystalline ZnO:Mn. Polarization dependence of the NEXAFS spectra from the PLD thin film with 5 at.%Mn is quantitatively reproduced by the present calculations. This suggests that Mn substitutes for Zn in ZnO and no significant precipitation takes place. This type of combination of the experimental and theoretical NEXAFS analysis with the assistance of XRD must be a powerful tool to investigate the local environment of transition metal dopants in DMSs.

This work was supported by three projects by Japanese Ministry of Education, Culture, Sports, Science and Technology (MEXT). They are the Computational Materials Science Unit in Kyoto University, the Grant-in-Aid for Scientific Research on Priority Areas (No. 751), and the 21st Century COE Program. Experimental supports by Dr. T. Okajima of Saga Light Source and T. Uruga of JASRI/SPring8 are gratefully acknowledged under Proposal No. 2003B0518-NXa-np and 2004A0401-NXa-np.

[1] H. Munekata, H. Ohno, S. von Molnar, A. Segmüller, L. L. Chang, and L. Esaki, Phys. Rev. Lett. **63**, 1849 (1989).
[2] H. Ohno, A. Shen, F. Matsukura, A. Oiwa, A. Endo, S. Katsumoto, and I. Iye, Appl. Phys. Lett. **69**, 363 (1996).
[3] T. Dietl, H. Ohno, F. Matsukura, J. Cibert, and D. Ferrand, Science **287**, 1019 (2000).
[4] P. Sharma, A. Gupta, K. V. Rao, F. J. Owens, R. Sharma, R. Ahuja, J. M. Osorio Guillen, B. Johansson, and G. A. Gehring, Nat. Mater. **2**, 673 (2003).
[5] S.-W. Lim, M.-C. Jeong, M.-H. Ham, and J.-M. Myoung, Jpn. J. Appl. Phys., Part 2 **43**, L280 (2004).
[6] Y. W. Heo, M. P. Ivill, K. Ip, D. P. Norton, S. J. Pearton, J. G. Kelly, R. Rairigh, A. F. Hebard, and T. Steiner, Appl. Phys. Lett. **84**, 2292 (2004).
[7] S. W. Jung, S.-J. An, G.-C. Yi, C. U. Jung, S.-I. Lee, and S. Cho, Appl. Phys. Lett. **80**, 4561 (2002).
[8] S. S. Kim, J. H. Moon, B.-T. Lee, O. S. Song, and J. H. Je, J. Appl. Phys. **95**, 454 (2004).
[9] T. Fukumura, Z. W. Jin, M. Kawasaki, T. Shono, T. Hasegawa, S. Koshihara, and H. Koinuma, Appl. Phys. Lett. **78**, 958 (2001).
[10] I. Tanaka, T. Mizoguchi, M. Matsui, S. Yoshioka, H. Adachi, T. Yamamoto, T. Okajima, M. Umesaki, W. Y. Ching, Y. Inoue, M. Mizuno, H. Araki, and Y. Shirai, Nat. Mater. **2**, 541 (2003).
[11] J. Okabayashi, K. Ono, M. Mizoguchi, M. Oshima, S. S. Gupta, D. D. Sarma, T. Mizokawa, A. Fujimori, M. Yuri, C. T. Chen, T. Fukumura, M. Kawasaki, and H. Koinuma, J. Appl. Phys. **95**, 3573 (2004).
[12] M. Kunisu, I. Tanaka, T. Yamamoto, T. Suga, and T. Mizoguchi, J. Phys.: Condens. Matter **16**, 3801 (2004).
[13] P. Blaha, K. Schwarz, G. Madsen, D. Kvasicka, and J. Luitz, *WIEN2k, An Augmented Plane Wave + Local Orbital Program for Calculating Crystal Properties* (Karlheinz Schwarz, Techn. Universitat Wien, Austria, 2001). ISBN 3-9501031-1-2).
[14] J. P. Perdew, S. Burke, and M. Ernzerhof, Phys. Rev. Lett. **77**, 3865 (1996).
[15] Geometry change due to the Mn substitution in ZnO was examined with the plane-wave pseudopotential method using a 72-atom supercell, in which one Zn was replaced by Mn. Since resultant change in bond length is only +2%, geometry change is not considered in the present NEXAFS calculation.
[16] G. B. Jensen and O. V. Nielsen, J. Phys. C **7**, 409 (1974).